Applied Physics Express **10**, 062502 (2017)
https://doi.org/**10.7567/APEX.10.062502**

Polymer optical fiber tapering using hot water

Yosuke Mizuno[1]*, Hiroki Ujihara[1], Heeyoung Lee[1], Neisei Hayashi[2], and Kentaro Nakamura[1]

[1]*Institute of Innovative Research, Tokyo Institute of Technology, Yokohama 226-8503, Japan*
[2]*Research Center for Advanced Science and Technology, The University of Tokyo, Meguro, Tokyo 153-8904, Japan*

*E-mail: ymizuno@sonic.pi.titech.ac.jp

Received February 21, 2017; accepted May 3, 2017; published online May 19, 2017

We perform a pilot trial of highly convenient taper fabrication for polymer optical fibers (POFs) using hot water. A ∼380-mm-long POF taper is successfully fabricated, and its ∼150-mm-long waist has a uniform outer diameter of ∼230 μm. The shape is in good agreement with the theoretical prediction. The optical loss dependence on the strain applied to the waist shows an interesting behavior exhibiting three regimes, the origins of which are inferred by microscopic observations. We then discuss the controllability of the taper length.

Brillouin scattering in optical fibers[1)] has been exploited to develop various devices such as strain and temperature sensors.[2–8)] To improve their performance, the Brillouin scattering properties in some special glass fibers have been investigated.[9,10)] However, as glass fibers are fragile and break at relatively small strains [∼3% for silica single-mode fibers (SMFs)], they cannot be directly used to measure larger strains. One method of tackling this problem is to use polymer optical fibers (POFs), which are so flexible that they can withstand even over 100% strain.[11)]

Several types of POFs are currently commercially available. The most widely used type is poly(methyl methacrylate)-based (PMMA-) step-index POFs,[12)] which mainly transmit visible light. However, Brillouin scattering in PMMA-POFs has not yet been experimentally observed because some of the optical devices necessary for Brillouin measurement are not commercially available at visible wavelengths. Another type widely used in laboratories is perfluorinated graded-index (PFGI-) POFs[13)] that are composed of cyclic transparent optical polymer (CYTOP) and transmit not only visible light but also telecom wavelength light. As many kinds of optical devices can be used at telecom wavelengths, Brillouin scattering in PFGI-POFs has already been experimentally observed.[14)] To date, we have investigated its physical properties at 1.55 μm, including the gain coefficient,[14)] threshold power,[14)] Brillouin frequency shift (BFS),[14)] and the BFS dependences on strain[15,16)] and temperature,[15)] proving its applicability to high-sensitivity temperature sensing[15)] and large-strain sensing.[16)] Meanwhile, one serious demerit of PFGI-POFs in Brillouin sensing applications is that the Brillouin Stokes power is relatively low because of their large core diameters (50–120 μm).[14)] The Stokes power in PFGI-POFs should be enhanced to implement sensors with a high signal-to-noise ratio.[17)]

One simple method of enhancing the Stokes power in PFGI-POFs is to increase the incident light power, the maximal limit of which is, however, much lower than that of silica SMFs. This is because the threshold power of the optical fiber fuse in PFGI-POFs is relatively low.[18,19)] Another method is to induce stimulated Brillouin scattering by a pump–probe technique,[20)] which is suitable for two-end-access sensing systems[2,4,6,21,22)] but cannot be directly employed in single-end-access systems.[3,5,7,8,23)] The combined use of pulsed pump light and a low-power optical amplifier is also known to be an effective method of enhancing the Stokes power,[24)] but it is not compatible with continuous wave (CW)-based sensing systems.[4–8,23)] Thus, to enhance the Stokes power in CW-based one-end-access sensing systems, such as Brillouin optical correlation-domain reflectometry,[7,8,23)] yet another method is desirable. For this purpose, here, we focus on the use of long tapered PFGI-POFs, which can enhance the Stokes power (generated at the tapered section), because the optical power density at the core center increases.[25)]

To date, many kinds of tapering techniques have been demonstrated.[26–41)] Among them, what we call a heat-and-pull technique has been most widely used to taper optical fibers, including glass fibers,[26–32)] PMMA-POFs,[33,34)] and PFGI-POFs.[25,35–37)] Many kinds of heat sources have been used for heating fibers, including a flame,[25–29)] a CO_2 laser,[30)] a compact furnace,[31,33–36)] a fusion splicer,[32)] and a solder gun,[37)] but these are sometimes not easy to handle, prepare, or control. To overcome this inconvenience in tapering POFs, hot water appears to be a good candidate as a heat source, because the glass-transition temperature of POFs is relatively low (∼100 °C).[42)] Besides, as heat is applied to the POFs almost uniformly (both radially and longitudinally) in hot water, its higher controllability might facilitate the fabrication of long tapered POFs. However, no papers regarding the tapering of POFs using hot water have yet been published.

In this paper, as a pilot trial, we demonstrate the heat-and-pull fabrication of PFGI-POF tapers using hot water as a heat source. In an experiment, a ∼380-mm-long PFGI-POF taper with a ∼150-mm-long waist is successfully fabricated. The waist has an almost uniform outer diameter of ∼230 μm, and this geometry agrees well with the theoretical prediction. During fabrication, the optical propagation loss is measured as a function of strain applied to the waist. It exhibits an interesting behavior containing three regimes, the origins of which are experimentally investigated.

The PFGI-POFs (Asahi Glass Fontex) tapered in this experiment have a three-layered structure: core (diameter: 50 μm; refractive index: ∼1.36), cladding (diameter: 70 μm), and overcladding (diameter: 490 μm). The core and cladding consist of doped and undoped CYTOP, respectively, the water absorption of which is negligibly small,[43)] and the overcladding is composed of polycarbonate. The optical propagation loss is relatively low (∼0.25 dB/m) even at 1.55 μm. The length of the PFGI-POF samples was 800 mm.

The experimental setup is depicted in Fig. 1. The output of a semiconductor laser at 1550 nm (power: 10 dBm) was injected into one end of a PFGI-POF via a silica SMF (butt-coupled),[14)] and the transmitted light was directly guided to an optical power meter. The room temperature was 18 °C. First, a 150-mm-long section around the midpoint of the

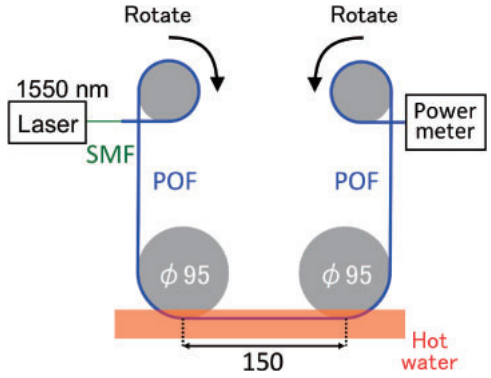

Fig. 1. Schematic of the POF tapering setup using hot water.

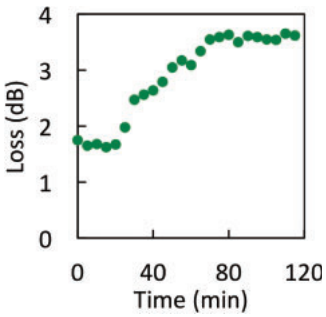

Fig. 2. Temporal variation in the propagation loss after the POF was partially immersed in hot water.

PFGI-POF was immersed in hot water (maintained at 97 °C) in a round vessel (diameter: 300 mm), and the temporal variation in the transmitted power was monitored until the power became almost constant. Subsequently, the PFGI-POF was pulled (or in other words, strained) in both directions via pulleys (diameter: 95 mm) at a rate of 0.50 mm/s (0.25 mm/s for each direction) until the PFGI-POF was completely cut. The transmitted power was also monitored during the pulling process. The same experiments were performed using other PFGI-POF samples with different pulling periods (pulling stopped before the samples were cut), and the tapered sections were observed using an optical microscope.

Figure 2 shows the temporal variation in the total optical loss after the 150-mm-long section of the PFGI-POF was immersed in hot water. The loss increased with time (probably caused by thermal shrinkage),[44] and approximately 80 min later, it became almost constant at ~3.6 dB.

Figure 3 shows the optical loss plotted as a function of the strain ε applied to the taper waist, which can be calculated as follows. Under the assumption that the volume of a fiber is maintained before and after the tapering process, it follows by simple calculation (see the online supplementary data at http://stacks.iop.org/APEX/10/062502/mmedia) that the strain ε applied to the taper waist is given by

$$\varepsilon = e^{D/L_w} - 1, \quad (1)$$

where D is the total pulled length in both directions, and L_w is the length of the fiber section immersed in hot water (150 mm in this experiment). As seen in Fig. 3, the loss remained unchanged for strains of less than ~100%. For larger strains of up to ~400%, the loss increased with a coefficient of ~0.010 dB/%. For even larger strains, the loss increased markedly with a coefficient of ~0.048 dB/%, and the PFGI-POF was completely cut at its midpoint when the strain

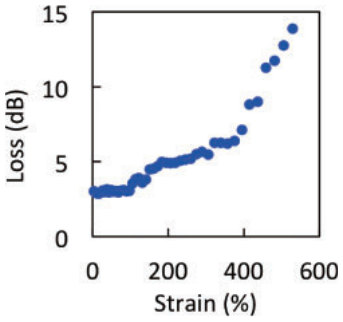

Fig. 3. Propagation loss of the tapered POF plotted as a function of the strain applied to the waist.

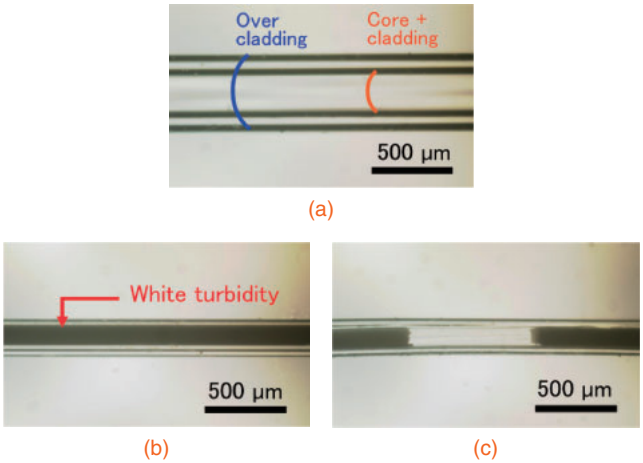

Fig. 4. Micrographs of the tapered POFs: (a) untapered section, (b) waist (strain: 360%), and (c) waist (strain: 500%).

reached ~560%. Thus, the dependence of loss on the strain exhibited three regimes, the origin of which is discussed in the following paragraph.

Another PFGI-POF sample was tapered in the same manner, and when the strain was 360%, it was removed from the hot water. The loss was 7.2 dB. Figures 4(a) and 4(b) show the micrographs of the untapered section and the taper waist, respectively. In Fig. 4(a), the core and cladding (their boundary is not visible) as well as the overcladding were transparent, whereas in Fig. 4(b), the core and cladding showed white turbidity caused by a phenomenon called crazing (i.e., the stress concentration causes nanoscale voids to form in the polymer, whereby light is scattered, resulting in whitening).[45] The distribution of the outer diameter along the length measured with a microscope is shown in Fig. 5. A ~380-mm-long section was tapered, and the outer diameter of the ~150-mm-long waist around its midpoint was approximately 230 μm, which was relatively uniform with a standard deviation of ~4 μm. This shape is in good agreement with the theoretical trend indicated by the solid curve [calculated using Eq. (1) (see the online supplementary data at http://stacks.iop.org/APEX/10/062502/mmedia); theoretical outer diameter of the waist: 233 μm]. The sections that were not immersed in hot water at all should be nontapered, but actually, they were slightly tapered, because the vapor from the hot water served as a heat source. This could be mitigated by thermally shielding part of the PFGI-POF. Subsequently, yet another PFGI-POF sample was also tapered at 500% strain. The micrograph of the midpoint of

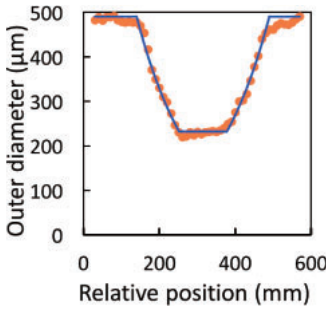

Fig. 5. Outer diameter distribution of the tapered POF (strain: 360%). The solid curve shows the theoretical trend.

the waist is shown in Fig. 4(c). The turbid core and cladding were cut, and only the overcladding maintained the fiber shape. On the basis of the aforementioned experimental observations, we can infer the origins of the three regimes of the dependence of loss on strain. Namely, the change at ~100% strain corresponds to the start of the white turbidity of the core and cladding, that at ~400% strain to the breakage of the turbid core and cladding, and that at ~560% strain to the breakage of the overcladding.

Finally, we discuss the length of the PFGI-POF tapers fabricated by this technique. As mentioned above, longer PFGI-POF tapers are desirable for Brillouin sensing applications. If the PFGI-POFs are pulled equally in both directions, the resultant tapered length is determined by the initial length of the PFGI-POF section immersed in hot water. Therefore, if a larger (or longer) vessel is used, longer PFGI-POF tapers can be easily fabricated. Even when the size of the vessel is fixed, we expect that much longer PFGI-POF tapers can be obtained if we give a new twist to the pulling structure. For instance, if one end of the PFGI-POF is pulled at 0.75 mm/s and the other end is pushed at 0.25 mm/s, the PFGI-POF is actually pulled at a rate of 0.50 mm/s while the pulled section is scanned along the PFGI-POF. This scheme may result in an extremely long PFGI-POF taper with high uniformity. Further study is required on this point.

In conclusion, we performed a pilot trial of taper fabrication for PFGI-POFs using hot water. We experimentally fabricated a ~380-mm-long PFGI-POF taper with a ~150-mm-long waist, the outer diameter of which was uniform (~230 μm). The geometry was in good agreement with the theory. The optical loss had an interesting dependence on the strain applied to the waist, containing three regimes, the mechanism of which was elucidated by microscopic observations. We also discussed the method of elongating the PFGI-POF tapers. Compared with other tapering techniques, our technique using hot water potentially has the advantages of ease of handling, cost efficiency, safety (no chemicals used), and high controllability of the length; thus, we consider that long PFGI-POF tapers fabricated by our technique will be a powerful tool for enhancing the signal-to-noise ratio of POF-based distributed Brillouin sensors in the future.

Acknowledgments This work was supported by JSPS KAKENHI Grant Numbers 25709032, 26630180, 25007652, and 17H04930 and by research grants from the Japan Gas Association, the ESPEC Foundation for Global Environment Research and Technology, and the Association for Disaster Prevention Research.

1) G. P. Agrawal, *Nonlinear Fiber Optics* (Academic Press, San Diego, CA, 1995).
2) T. Horiguchi and M. Tateda, J. Lightwave Technol. **7**, 1170 (1989).
3) T. Kurashima, T. Horiguchi, H. Izumita, S. Furukawa, and Y. Koyamada, IEICE Trans. Commun. **E76-B**, 382 (1993).
4) D. Garus, K. Krebber, F. Schliep, and T. Gogolla, Opt. Lett. **21**, 1402 (1996).
5) A. Minardo, R. Bernini, R. Ruiz-Lombera, J. Mirapeix, J. M. Lopez-Higuera, and L. Zeni, Opt. Express **24**, 29994 (2016).
6) K. Hotate and T. Hasegawa, IEICE Trans. Electron. **E83-C**, 405 (2000).
7) Y. Mizuno, W. Zou, Z. He, and K. Hotate, Opt. Express **16**, 12148 (2008).
8) Y. Mizuno, W. Zou, Z. He, and K. Hotate, J. Lightwave Technol. **28**, 3300 (2010).
9) K. S. Abedin, Opt. Express **13**, 10266 (2005).
10) Y. Mizuno, N. Hayashi, and K. Nakamura, J. Appl. Phys. **112**, 043109 (2012).
11) H. Ujihara, N. Hayashi, M. Tabaru, Y. Mizuno, and K. Nakamura, IEICE Electron. Express **11**, 20140707 (2014).
12) M. G. Kuzyk, *Polymer Fiber Optics: Materials, Physics, and Applications* (CRC Press, Boca Raton, FL, 2006).
13) Y. Koike and M. Asai, NPG Asia Mater. **1**, 22 (2009).
14) Y. Mizuno and K. Nakamura, Appl. Phys. Lett. **97**, 021103 (2010).
15) Y. Mizuno and K. Nakamura, Opt. Lett. **35**, 3985 (2010).
16) N. Hayashi, Y. Mizuno, and K. Nakamura, Opt. Express **20**, 21101 (2012).
17) N. Hayashi, Y. Mizuno, and K. Nakamura, J. Lightwave Technol. **32**, 3397 (2014).
18) Y. Mizuno, N. Hayashi, H. Tanaka, K. Nakamura, and S. Todoroki, Appl. Phys. Lett. **104**, 043302 (2014).
19) Y. Mizuno, N. Hayashi, H. Tanaka, K. Nakamura, and S. Todoroki, Sci. Rep. **4**, 4800 (2014).
20) Y. Mizuno, M. Kishi, K. Hotate, T. Ishigure, and K. Nakamura, Opt. Lett. **36**, 2378 (2011).
21) A. Denisov, M. A. Soto, and L. Thévenaz, Light: Sci. Appl. **5**, e16074 (2016).
22) D. Zhou, Y. Dong, B. Wang, T. Jiang, D. Ba, P. Xu, H. Zhang, Z. Lu, and H. Li, Opt. Express **25**, 1889 (2017).
23) Y. Mizuno, N. Hayashi, H. Fukuda, K. Y. Song, and K. Nakamura, Light: Sci. Appl. **5**, e16184 (2016).
24) Y. Mizuno and K. Nakamura, Appl. Phys. Express **5**, 032501 (2012).
25) N. Hayashi, H. Fukuda, Y. Mizuno, and K. Nakamura, J. Appl. Phys. **115**, 173108 (2014).
26) J. C. Knight, G. Cheung, F. Jacques, and T. A. Birks, Opt. Lett. **22**, 1129 (1997).
27) T. A. Birks, W. J. Wadsworth, and P. St. J. Russel, Opt. Lett. **25**, 1415 (2000).
28) L. Tong, R. R. Gattass, J. B. Ashcom, S. He, J. Lou, M. Shen, I. Maxwell, and E. Mazur, Nature **426**, 816 (2003).
29) G. Brambilla, V. Finazzi, and D. J. Richardson, Opt. Express **12**, 2258 (2004).
30) T. E. Dimmick, G. Kakarantzas, T. A. Birks, and P. St. J. Russell, Appl. Opt. **38**, 6845 (1999).
31) M. Sumetsky, Y. Dulashko, and A. Hale, Opt. Express **12**, 3521 (2004).
32) F. Lissillour, D. Messager, G. Stéphan, and P. Féron, Opt. Lett. **26**, 1051 (2001).
33) Y. Jeong, S. Bae, and K. Oh, Curr. Appl. Phys. **9**, e273 (2009).
34) D. J. Feng, G. X. Liu, X. L. Liu, M. S. Jiang, and Q. M. Mei, Appl. Opt. **53**, 2007 (2014).
35) J. Arrue, F. Jiménez, G. Aldabaldetreku, G. Durana, J. Zubia, M. Lomer, and J. Mateo, Opt. Express **16**, 16616 (2008).
36) R. Gravina, G. Testa, and R. Bernini, Sensors **9**, 10423 (2009).
37) A. A. Jasim, N. Hayashi, S. W. Harun, H. Ahmad, R. Penny, Y. Mizuno, and K. Nakamura, Sens. Actuators A **219**, 94 (2014).
38) D. F. Merchant, P. J. Scully, and N. F. Schmitt, Sens. Actuators A **76**, 365 (1999).
39) H. Ujihara, N. Hayashi, K. Minakawa, Y. Mizuno, and K. Nakamura, Appl. Phys. Express **8**, 072501 (2015).
40) H. Lee, N. Hayashi, Y. Mizuno, and K. Nakamura, Jpn. J. Appl. Phys. **54**, 118001 (2015).
41) S. Shimada, H. Lee, M. Shizuka, H. Tanaka, N. Hayashi, Y. Matsumoto, Y. Tanaka, H. Nakamura, Y. Mizuno, and K. Nakamura, Appl. Phys. Express **10**, 012201 (2017).
42) K. Koike, H. Teng, Y. Koike, and Y. Okamoto, Polym. Adv. Technol. **25**, 204 (2014).
43) S. Ando, T. Matsuura, and S. Sasaki, Chemtech **24**, 20 (1994).
44) V. A. Beloshenko, Y. E. Beygelzimer, and V. N. Varyukhin, Polymer **41**, 3837 (2000).
45) Z. M. Xiao, M. K. Lim, and K. M. Liew, J. Mater. Process. Technol. **48**, 437 (1995).